E&G Quaternary Sci. J., 66, 91–100, 2017
https://doi.org/10.5194/egqsj-66-91-2017


Open Access E&G Quaternary Science Journal

Research article

# Late Quaternary climate and environmental reconstruction based on leaf wax analyses in the loess sequence of Möhlin, Switzerland

**Lorenz Wüthrich[1,2], Marcel Bliedtner[1,2], Imke Kathrin Schäfer[1,2], Jana Zech[1], Fatemeh Shajari[3], Dorian Gaar[2,4], Frank Preusser[5], Gary Salazar[2,6], Sönke Szidat[2,6], and Roland Zech[1,2]**

[1]Geographical Institute, University of Bern, Bern, Switzerland
[2]Oeschger Centre for Climate Change Research, University of Bern, Bern, Switzerland
[3]Geo and Environmental Engineering, Technical University of Munich, Munich, Germany
[4]Institute of Geology, University of Bern, Bern, Switzerland
[5]Institute of Earth and Environmental Sciences, University of Freiburg, Freiburg, Germany
[6]Department of Chemistry and Biochemistry, University of Bern, Bern, Switzerland

**Correspondence:** Lorenz Wüthrich (loeru@live.com)

**Relevant dates:** Published: 21 December 2017

**How to cite:** Wüthrich, L., Bliedtner, M., Schäfer, I. K., Zech, J., Shajari, F., Gaar, D., Preusser, F., Salazar, G., Szidat, S., and Zech, R.: Late Quaternary climate and environmental reconstruction based on leaf wax analyses in the loess sequence of Möhlin, Switzerland, E&G Quaternary Sci. J., 66, 91–100, https://doi.org/10.5194/egqsj-66-91-2017, 2017.

**Abstract:** We present the results of leaf wax analyses (long-chain *n*-alkanes) from the 6.8 m deep loess sequence of Möhlin, Switzerland, spanning the last ∼70 kyr. Leaf waxes are well preserved and occur in sufficient amounts only down to 0.4 m and below 1.8 m depth, so no paleoenvironmental reconstructions can be done for marine isotope stage (MIS) 2.

Compound-specific $\delta^2H_{wax}$ analyses yielded similar values for late MIS 3 compared to the uppermost samples, indicating that various effects (e.g., more negative values due to lower temperatures, more positive values due to an enriched moisture source) cancel each other out. A pronounced ∼30 ‰ shift towards more negative values probably reflects more humid conditions before ∼32 ka. Radiocarbon dating of the *n*-alkanes corroborates the stratigraphic integrity of leaf waxes and their potential for dating loess–paleosol sequences (LPS) back to ∼30 ka.

**Kurzfassung:** Wir präsentieren die Ergebnisse von Blattwachsanalysen (langkettige *n*-Alkane) aus einer 6.8 m mächtigen Löss-Sequenz bei Möhlin, Schweiz, welche bis etwa 70 ka zurückreicht. Nur bis 0.4 m Tiefe und unterhalb von 1.8 m sind die Blattwachse gut und in ausreichender Menge erhalten, so dass Aussagen bezüglich der Umweltbedingungen während der marinen Isotopenstufe (MIS) 2 nicht gemacht werden können. Die Muster der *n*-Alkane zeigen für alle Proben einen dominanten Input von Gras-Alkanen, jedoch ist es nur anhand der *n*-Alkane nicht möglich, die Existenz von Koniferen vor allem während des MIS 3 auszuschliessen. Komponenten-spezifische $\delta^2H_{wax}$ Analysen zeigen für MIS 3 ähnliche Werte wie für die obersten Proben aus der Sequenz. Offensichtlich heben sich mehrere Effekte gegenseitig auf (z.B. negativere Werte aufgrund niedrigerer Temperatur, positivere Werte aufgrund angereicherter Feuchtigkeitsquellen). Ein auffälliger ∼30 ‰ Wechsel zu negativeren Werten

zeigt vermutlich feuchtere Bedingungen vor ∼ 32 ka an. Komponenten-spezifische Radiokohlenstoff-Datierungen bestätigen die stratigraphische Integrität der Blattwachse und untermauern ihr Potential für die Datierung von Löss-Paläoboden Sequenzen bis etwa 30 ka.

## 1 Introduction

Vast parts of Switzerland were repeatedly covered by glaciers (Graf, 2009). This explains the lack of widespread thick loess deposits as they exist, for example, in southeastern Germany, southeastern and eastern Europe (Haase et al., 2007). Nevertheless, there are a few sites in Switzerland where loess has been found (Gouda, 1962; Preusser et al., 2011; Gaar and Preusser, 2017), and they might have potential for paleoenvironmental reconstruction. One of these sites is the Möhliner Feld in northwestern Switzerland (Fig. 1). Until recently, there was a subdued ridge considered to be a terminal moraine of the most extensive glaciation (MEG; > 300 ka) in the Swiss Alps (Gutzwiler, 1894; Penck and Brückner, 1909; Keller and Krayss, 2011). However, the ridge cannot be linked to the MEG, because till containing Alpine material is only found 30 m below the surface and covered by gravel and loess (Preusser et al., 2011; Gaar and Preusser, 2017). While the till can be attributed to the MEG, although no numerical age control is available, the ridge has to be interpreted as a loess dune, not as a moraine, as it consists of loess (Gaar and Preusser, 2017). The dune might have been deposited by strong winds, called the "Möhlin jet". The jet nowadays mostly occurs in winter, when the air fills up the Swiss Plateau and overflows the eastern Jura Mountains. This results in a dry wind with a speed of up to 10 m $s^{-1}$ (Schüepp, 1982; Müller, 2001; Gaar and Preusser, 2017). In 2011, a rotary drill core was recovered from the ridge, consisting entirely of loess sediment down to 6.8 m depth. According to luminescence dating (OSL and IR50), most of the loess was deposited during marine isotope stage (MIS) 2 and late MIS 3, while the lowermost part of the sequence probably dates back to MIS 4 (Gaar and Preusser, 2017).

For the present study, we analyzed long-chain *n*-alkanes, i.e., leaf waxes, in the drill core from Möhlin in order to evaluate their potential for paleovegetation reconstruction. Moreover, we applied compound-specific $\delta^2$H analyses on the most abundant *n*-alkanes (*n*-$C_{29}$ and *n*-$C_{31}$) to reconstruct paleoclimate and hydrology. In addition, we performed radiocarbon dating on some *n*-alkane samples to test the stratigraphic integrity of the leaf waxes.

## 2 Leaf waxes – a novel tool in Quaternary research

Long-chain *n*-alkanes (> *n*-$C_{25}$) are produced by higher terrestrial plants (de Bary, 1871; Eglinton and Hamilton, 1963, 1967; Kunst, 2003; Shepherd and Wynne Griffiths, 2006; Samuels et al., 2008). They are straight, saturated

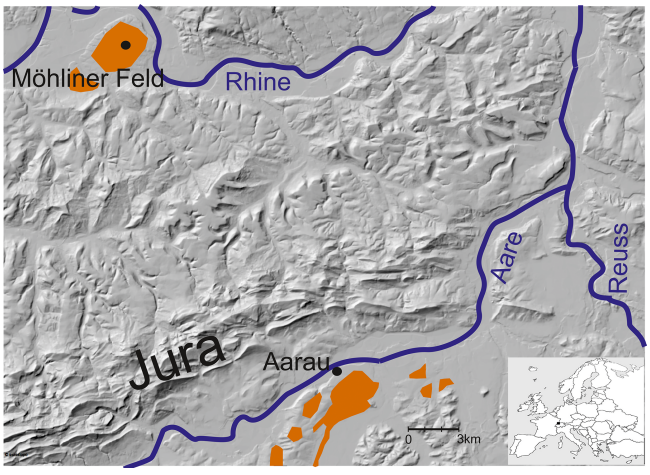


**Figure 1.** Research area. Orange fields mark loess deposits, drawn after Gouda (1962). Source hillshade: Federal Office of Topography.

carbon–hydrogen chains ($C_nH_{2n+2}$), stable over geological timescales (Eglinton and Eglinton, 2008; Schimmelmann et al., 2006) and thus preserved in various sedimentary archives. Their homologue pattern depends on the type of vegetation (Cranwell, 1973; Marseille et al., 1999; Schwark et al., 2002) and can provide information about whether deciduous trees or grasses were dominant in the research area, whereas deciduous trees produce mainly *n*-$C_{27}$ and grasses predominantly *n*-$C_{31}$ and *n*-$C_{33}$ (Zech et al., 2010; Schäfer et al., 2016b; Schwark et al., 2002). Although controversy exists as to whether this approach can be used universally to reconstruct paleovegetation (Bush and McInerney, 2013; Wang et al., 2015), there is good evidence that leaf wax patterns can be used on a local (Schwark et al., 2002) and regional (Schäfer et al., 2016a) scale in Europe. Schwark et al. (2002) investigated *n*-alkanes in a lake in southern Germany and found a remarkable accordance of pollen records and *n*-alkanes. Schäfer et al. (2016a) measured leaf wax patterns along a transect from southern to northern Europe in grasslands, deciduous forests and coniferous forests. They analyzed samples from litter and two depths of the uppermost soil horizon. The results of the Schäfer et al. (2016a) study are that (1) the chain lengths correlate significantly along the transect with the grassland and deciduous vegetation, (2) *n*-alkanes from conifer forests show the understorey and (3) a correction for degradation of the *n*-alkanes is needed to get reliable information about the vegetation. *n*-Alkane patterns are thus a particularly valuable tool for the reconstruction of

paleovegetation when pollen are absent, which is often the case in loess–paleosol sequences (LPS).

The compound-specific isotopic composition of *n*-alkanes ($\delta^2H_{wax}$) is increasingly used as a tool for the reconstruction of past climate conditions. Liu and Huang (2005) measured $\delta^2H_{wax}$ in a Chinese loess–paleosol sequence and showed that it recorded past climate changes. In principle, $\delta^2H_{wax}$ reflects the isotopic composition of precipitation ($\delta^2H_{precip}$) (Sachse et al., 2012), which in turn depends on (and is thus a proxy for) climate (temperature, precipitation amount, evaporation) and geographical location (latitude, altitude, continentality, moisture source) (Dansgaard, 1964). Additional factors that need to be taken into account when interpreting $\delta^2H_{wax}$ records are biosynthetic fractionation, evapotranspirative enrichment, vegetation period, degradation and type of vegetation (Sessions et al., 1999; Sachse et al., 2006; M. Zech et al., 2011, 2015; Kahmen et al., 2013; Gao et al., 2014; Hepp et al., 2015; Tipple et al., 2013). Evapotranspiration leads to an enrichment, depending mainly on relative humidity (M. Zech et al., 2013; Farquhar et al., 2007). Biosynthetic fractionation is often assumed to be $\sim 160\,‰$ (Sachse et al., 2012).

Compound-specific radiocarbon analyses on sedimentary *n*-alkanes is a new tool in geochronology (Häggi et al., 2014; Haas et al., 2017; Zech et al., 2017). It allows us to test the synsedimentary nature, and thus the stratigraphic integrity of leaf waxes, and can complement other dating methods, for example based on luminescence.

## 3 Material and methods

The drill core from Möhlin is described in detail in Gaar and Preusser (2017). In brief, the core consists of loess down to 6.8 m but is decalcified and overprinted by pedogenesis down to 1.6 m depth and from 5.9 to 6.2 m. We sampled the core in continuous 20 cm intervals for leaf wax analyses.

### 3.1 Leaf wax analyses

Approximately 40 g of each sample was extracted with an accelerated solvent extractor using dichloromethane / methanol (9/1). The total lipid extract was dried and passed over pipette columns with an aminopropyl-coated silica gel as the stationary phase. Nonpolar compounds, including *n*-alkanes, were eluted with hexane and then spiked with 5$\alpha$-androstane. The long-chain *n*-alkanes ($nC_{25}$–$nC_{35}$) were analyzed using a GC-FID (gas chromatography–flame ionization detector) at the Department of Soil Science at TUM-Weihenstephan, Freising, Germany. The Thermo Scientific Trace 1310 was equipped with a Zebron ZB-5HT column and operated in splitless injection mode. The He carrier gas flow was set constantly to 1.2 mL min$^{-1}$, and the GC temperature was first held at 50 °C for 1 min, ramped to 250 °C at 30 °C min$^{-1}$ and then to 340 °C at 7 °C min$^{-1}$, and held for 11 min.

The most abundant *n*-alkanes, $nC_{29}$ and $nC_{31}$, were later targeted at the Geographical Institute, University of Bern, for compound-specific $\delta^2H$ analyses. Using an IsoPrime 100 mass spectrometer, coupled to an Agilent 7890A GC via a GC5 pyrolysis–combustion interface operating in pyrolysis mode with a Cr (ChromeHD) reactor at 1000 °C. Each sample was measured three times. Precision of the measurements was checked by analyzing a standard *n*-alkane mixture with known isotopic composition twice every six runs. The $H_3+$ factor was 3.4 and stable. The results are given in delta notation ($\delta^2H$) versus Vienna Standard Mean Ocean Water (VSMOW).

### 3.2 *n*-Alkane patterns

The total *n*-alkane concentration (µg g$^{-1}$ dry weight, $A_{tot}$) is here defined as the sum of $nC_{25}$ to $nC_{35}$. The odd-over-even predominance (OEP; Eq. 1) was calculated after Hoefs et al. (2002) and is an indicator for degradation: values smaller than 5 are considered to be strongly degraded (Zech et al., 2010; Schäfer et al., 2016a) and must thus be interpreted with care.

$$\mathrm{OEP} = \frac{nC_{27} + nC_{29} + nC_{31} + nC_{33}}{nC_{26} + nC_{28} + nC_{30} + nC_{32}} \quad (1)$$

Changes in the average chain length (ACL; Eq. 2) of the measured *n*-alkanes indicate whether deciduous trees and shrubs (shorter ACL) or grasses and herbs (longer ACL) were the dominant plant type (Poynter et al., 1989).

$$\mathrm{ACL} = \frac{27 \cdot nC_{27} + 29 \cdot nC_{29} + 31 \cdot nC_{31} + 33 \cdot nC_{33}}{nC_{27} + nC_{29} + nC_{31} + nC_{33}} \quad (2)$$

Because degradation can influence the ACL, one needs to correct for those effects (Zech et al., 2010). We performed a correction after Schäfer et al. (2016a) (Eq. 3–6), which results in the semi-quantitative %grass content for the samples.

$$\text{Tree endmember} = 0.09 \cdot \ln(\mathrm{OEP}) + 0.66 \quad (3)$$

$$\text{Grass endmember} = -0.17 \cdot \ln(\mathrm{OEP}) + 0.75 \quad (4)$$

$$\mathrm{Ratio} = \frac{n-C_{31} + n-C_{33}}{n-C_{27} + n-C_{31} + n-C_{33}} \quad (5)$$

$$\%\mathrm{Grass} = \frac{\text{ratio} - \text{tree endmember}}{\text{grass endmember} - \text{tree endmember}} \quad (6)$$

### 3.3 Radiocarbon dating

For radiocarbon analyses of the *n*-alkanes, four samples were selected and the nonpolar fraction passed over two pipette columns filled with $AgNO_3$ impregnated silica gel and zeolite, respectively. The zeolite was dissolved in HF, and the purified *n*-alkanes were recovered via liquid–liquid extraction with *n*-hexane. Finally, the purified *n*-alkanes were transferred with dichloromethane into tin capsules. The $^{14}C$ measurements were performed on the MICADAS accelerator mass spectrometer, coupled to an element analyzer (Ruff

et al., 2010; Salazar et al., 2015), at the LARA AMS Laboratory, University of Bern (Szidat et al., 2014). $^{14}C$ results are reported as fraction modern carbon ($F^{14}C$) and were corrected for constant and blank contamination (Salazar et al., 2015; Haas et al., 2017). The blank contamination was 0.4 µg C for a single tin capsule with a $F^{14}C$ value of $0.734 \pm 0.19$. The calibrated radiocarbon ages were calculated using OxCal (Ramsey, 2009) and IntCal13 (Reimer et al., 2013).

## 4 Results

Most samples from Möhlin are characterized by a dominance of odd, long-chain ($> nC_{25}$) *n*-alkanes typical for leaf waxes; additionally, other compounds and an unresolved matrix complex occur in variable amounts (Fig. 2).

However, samples from 0.4 to 1.6 m depth have very low concentrations and quantification of the target compounds is difficult. Total *n*-alkane concentrations for these samples can only be estimated as $< 0.4\ \mu g\ g^{-1}$, and the OEP values are less than 5, indicating enhanced degradation. These samples are therefore not plotted in Fig. 3. All other data are illustrated in Fig. 3, Table 1 and the supplement table (Wüthrich et al., 2017b).

The two uppermost samples have *n*-alkane concentrations of 1.2 and $0.4\ \mu g\ g^{-1}$, OEP values of 8.3 and 7.5, and ACL values of 30.1, respectively. Samples from depths of 1.6 to 6.8 m have highly variable *n*-alkane concentrations, ranging from 1 to $5.3\ \mu g\ g^{-1}$. Their OEP values range from 9.9 to 18.6, and their ACL is between 30.5 and 31.1. The uppermost two samples and the samples below 1.6 m depth had sufficient amounts of $nC_{29}$ and $nC_{31}$ for compound-specific $\delta^2H$ analyses. $\delta^2H_{wax}$ values range from −215.1 to −143.5 ‰ and from −210.4 to −146.9 ‰, respectively. Down-core patterns are very similar and correlate well with an *R* value of 0.68.

All four samples selected and purified for radiocarbon dating yielded sufficient carbon masses for AMS analyses (Table 4.1). Fraction modern ($F^{14}C$) ranges from 0.023 to 0.055, yielding calibrated $2\sigma$ ages between 26.4 and 38.0 cal kyr BP. As we did measure the whole *n*-alkane fraction and not single compounds, a contamination of post-sedimentary, especially short-chain and even-numbered, *n*-alkanes is possible, leading to too-young ages. But as three samples are in very good agreement with the ages published by Gaar and Preusser (2017), a contamination can most probably be excluded for the uppermost three samples.

## 5 Discussion

### 5.1 Chronology

The uppermost IR50 (infrared stimulated luminescence at 50°) and OSL (optically stimulated luminescence) ages from Gaar and Preusser (2017) suggest that at least the upper ~ 1 m of Möhlin sequence was deposited ~ 19 ka, i.e., MIS 2, and just before final deglaciation of the Swiss Plateau (Wirsig et al., 2016; Wüthrich et al., 2017a). Soil formation and decalcification down to 1.6 m depth must have occurred during the Late Glacial and Holocene. The next three IR50 and OSL ages from depths of 3.4 to 5 m document rapid sedimentation between 34 and 31 ka, i.e., late MIS 3. Our radiocarbon ages from depths of 2.0 and 3.4 m are slightly younger (26.4 to 30.0 cal kyr BP) but are in reasonable agreement in view of the limitations and uncertainties related to both the luminescence and the radiocarbon dating methods. The radiocarbon age from 5.8 m depth is 31.7 to 38.0 cal kyr BP and with only 0.023 $F^{14}C$ even closer to the lower limit of radiocarbon dating. Nevertheless, the age is also in good agreement with the OSL and IR50 ages of 31.0 and 41 kyr, respectively, from the same depth, so all of these ages document rapid loess accumulation during late MIS 3 (Fig. 3).

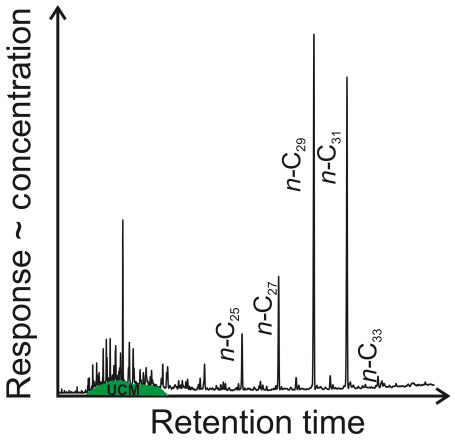


**Figure 2.** Example of a chromatogram (M13 from 2.4 m depth), showing the unresolved matrix complex (green) and the *n*-alkane compounds produced in leafs.

The weak paleosol preserved between 5.9 and 6.2 m depth must have developed earlier although probably still during MIS 3, because it developed into loess deposited during MIS 4 based on OSL and IR50 ages of 68.1 and 58.1 kyr, respectively. Our radiocarbon age from 6.8 m depth is only 28.7–32.2 cal kyr BP and very likely underestimates the real sedimentation age of the loess at this depth. The $F^{14}C$ of the sample is only 0.038 and the smallest amounts of contamination (in the lab or from other compounds) can readily explain the discrepancy between the luminescence and radiocarbon ages. Another possibility might be incorporation of root-derived *n*-alkanes by roots from plants growing after deposition, as suggested, for example, by Gocke et al. (2014). But a post-sedimentary production of roots can most probably be excluded, as shown by Häggi et al. (2014), Zech et al. (2017) and Haas et al. (2017).

In general, our radiocarbon results are in reasonable agreement with the ages of Gaar and Preusser (2017) and corrob-

**Table 1.** Radiocarbon data and ages for the four selected samples.

| Sample label | Sample code | Carbon mass (µg) | $F^{14}C$ | Age range ($2\sigma$) (cal kyr BP) |
|---|---|---|---|---|
| M11 | BE-3951.1.1 | 54 | $0.0547 \pm 0.0040$ | 26.4–28.7 |
| M18 | BE-3952.1.1 | 42 | $0.0486 \pm 0.0040$ | 27.4–30.0 |
| M31 | BE-3953.1.1 | 80 | $0.0229 \pm 0.0037$ | 31.7–38.0 |
| M36 | BE-3954.1.1 | 88 | $0.0378 \pm 0.0038$ | 28.7–32.2 |

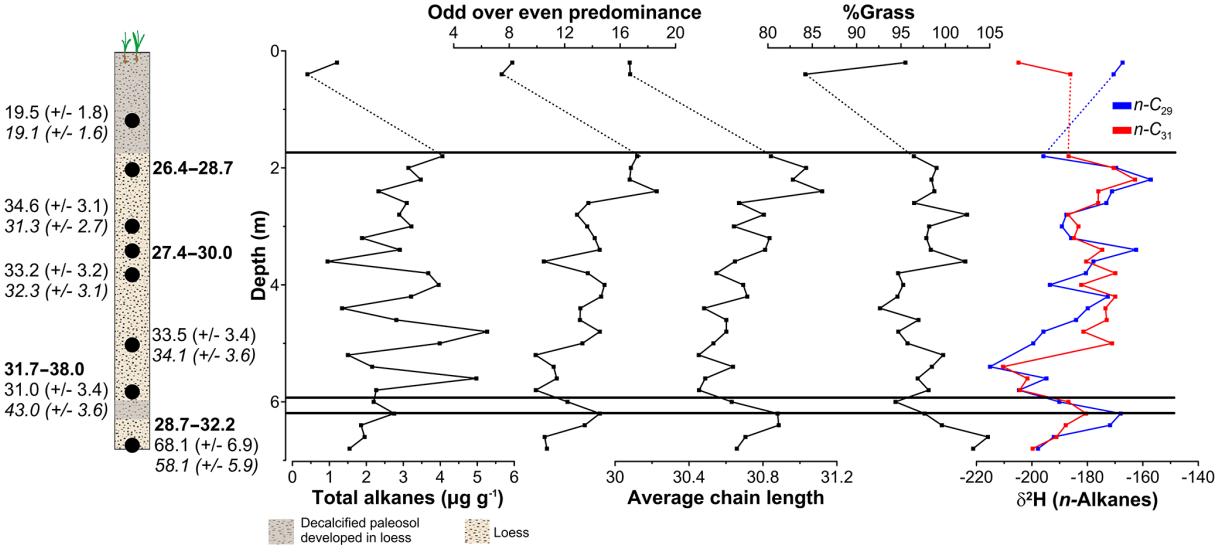


**Figure 3.** *n*-Alkane dates for the Möhlin loess sequence. OSL and IR50 (italic) ages have previously been published in Gaar and Preusser (2017); radiocarbon ages are given in bold letters.

orate that radiocarbon analyses of *n*-alkanes are a promising new tool for dating LPS back to ~30 ka (Häggi et al., 2014; Haas et al., 2017; Zech et al., 2017). Moreover, the stratigraphic integrity and synsedimentary nature of the long-chain *n*-alkanes could be confirmed for the uppermost 6 m.

The OSL, IR50 (Gaar and Preusser, 2017) and our radiocarbon ages show that the major part of the sequence was developed between 35 and 30 kyr and that older deposits are probably influenced by erosion. The paleosol might show a hiatus. Our interpretation is thus mainly valid for the time between 35 and 30 ka, when the rapid loess accumulation occurred.

## 5.2 Paleovegetation

The uppermost two samples from depths of 0.2 and 0.4 m have a relatively low ACL compared to most other samples from the profile. This indicates more input of *n*-alkanes from deciduous trees and shrubs; however, concentrations are also lower, and lower OEP values show enhanced degradation (Fig. 4). The plot also illustrates that changes in the alkane ratio (the same is true for the ACL) are partly an artefact of degradation. However, the sample from 0.4 m depth plots furthest below the grass endmember, which is numerically expressed as lowest %grass (Fig. 3). This possibly reflects the remnant leaf wax signal from the natural potential vegetation at Möhlin during the Holocene, i.e., mainly deciduous trees, whereas the site is used today as grassland.

While the *n*-alkanes between 0.6 and 1.6 m are strongly degraded and too low in concentration to robustly infer any paleoenvironmental conditions during MIS 2, high concentrations and good preservation allow this for the rest of the sequence. The positive trend in the ACL from depths of ~6 to 2 m indicates an increase of grass-derived *n*-alkane input during late MIS 3. However, the observed trend in ACL is probably an artefact of degradation. This is illustrated in the endmember again (Fig. 4), in which all these samples plot very close to the grass endmember. Accordingly, %grass (Fig. 3) does not show much of a trend and no major vegetation changes seem to be documented in the *n*-alkane patterns for the lower part of the profile between 1.8 and 6.8 m depth, i.e., during MIS 4 and MIS 3. This example shows that it is imperative to not over-interpret ACL and to account for degradation, even when preservation is generally good.

Our results suggest that the *n*-alkanes preserved at Möhlin during MIS 3 and possibly MIS 4 were mainly produced by grasses and herbs and that deciduous trees and shrubs

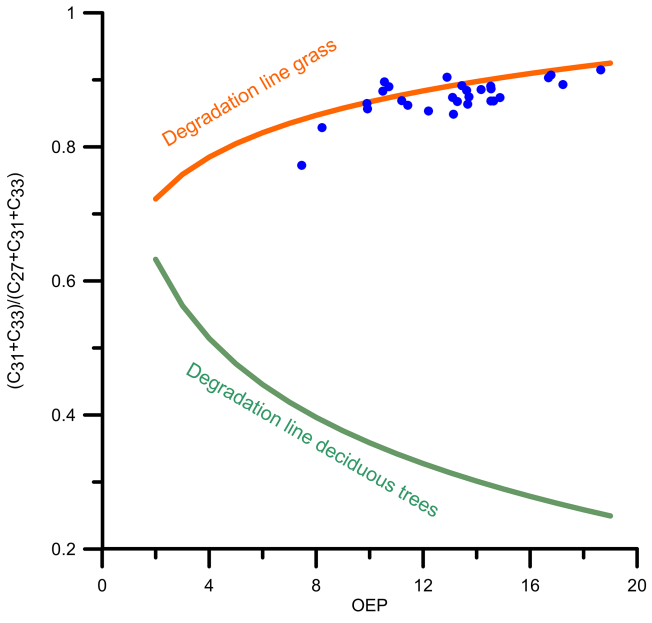


**Figure 4.** Endmember plot after Schäfer et al. (2016a). Our samples from Möhlin are plotted in blue.

played a minor role, if any. Based on *n*-alkanes only, however, one cannot rule out that conifer trees grew at the research site. *n*-Alkane concentrations in conifer needles are mostly about an order of magnitude lower than in deciduous trees or grass, with the exception of *Juniperus*. Hence *n*-alkane proxy records are quite insensitive for detecting conifer vegetation (Diefendorf et al., 2011; Tarasov et al., 2013; Schäfer et al., 2016b). Open conifer forest during parts of MIS 3 have been reported from peat sequences at Gossau (Schlüchter et al., 1987; Preusser et al., 2003) and Niederwenigen (Drescher-Schneider et al., 2007), both located a few dozen kilometers to the east of Möhlin. Similar vegetation may have prevailed at Möhlin, with the long-chain *n*-alkanes having only recorded thinly recorded grasses, i.e., the understory of the open conifer forest.

## 5.3 Paleoclimatology

The $\delta^2H_{wax}$ values from the uppermost two samples (ranging from −167 to −205 ‰; Fig. 3) are perfectly in the range observed in topsoil samples from central Europe (Schäfer et al., unpublished data) and in agreement with what can be expected based on theoretical considerations. Assuming a constant metabolic fractionation of −160 ‰, $\delta^2H_{leaf\,water}$ for the uppermost two samples ranges from −8.7 to −53.4 ‰. This is close but tends to be a little bit higher than today's $\delta^2H_{precip}$ in Möhlin, which has a value of ∼ −40 ‰ in summer (Bowen et al., 2005; Bowen, 2008). As spring and possibly also winter precipitation, which is more depleted than summer precipitation, may have been used by the plants as well, some evapotranspirative enrichment certainly occurred.

The $\delta^2H_{wax}$ values below 1.8 m depth are relatively constant around −180 ‰, i.e., similar to the values from the uppermost two samples. Most conspicuously, a sudden drop occurs just below 5 m depth to values as low as −215 ‰ (Fig. 3). $\delta^2H_{wax}$ then increases again in the lowermost meter of the Möhlin sequence. The observed $\delta^2H_{wax}$ pattern strongly resembles the pattern from the LPS Bobingen, Germany, 200 km northeast of Möhlin (R. Zech et al., 2015). Here, *n*-alkanes are ∼ −200 ‰ in sediments dated to latest MIS 3 (∼ 30 ka) and MIS 2, and values drop to < −220 ‰ below, before they increase again in the lowest part of the profile dated to ∼ 45 ka.

Overall, we are therefore confident that the $\delta^2H_{wax}$ record from Möhlin is a local signal but also carries valuable regional information about paleoclimate changes. Interpretation in terms of changes in $\delta^2H_{precip}$ and evapotranspirative enrichment is, however, very challenging because disentangling these two major controls is not yet possible. To the best of our knowledge, there are no independent continuous records of $\delta^2H_{precip}$ in Europe during the last glacial. Luetscher et al. (2015) presented a $\delta^{18}O$ record from a northern Alpine speleothem, but it overlaps only slightly with ours and shows very little variation from 30 to 15 ka (∼ 1 ‰ $\delta^{18}O$, which is equivalent to ∼ 8 ‰ $\delta^2H$). The only long continuous isotope records spanning the last 40 to 60 kyr currently come from an LPS in Crvenka, Serbia (R. Zech et al., 2013), which shows not much more than 10 ‰ variability, and from marine cores offshore Portugal (Abreu et al., 2003) and in the Mediterranean Sea (Frigola et al., 2008). The marine $\delta^{18}O$ records (measured on foraminifera) show a minor trend towards more enriched values (corresponding to a $\delta^2H$ trend < 10 ‰) from ∼ 60 to 20 ka. Afterwards, during the last glacial termination and the Holocene, values become much more negative (∼ 20 ‰ $\delta^2H$). A comparison of these records suggests the following hypotheses: the sudden enrichment in $\delta^2H_{wax}$ after 32 kyr does not reflect a sudden change in the source, i.e., the North Atlantic. It might therefore document a sudden onset of more arid conditions and enhanced evapotranspiration.

The interpretation of the uppermost two samples is trickier: on one hand, the elevated $\delta^2H_{wax}$ of $nC_{29}$ in the uppermost two samples in Möhlin might document even more arid conditions than during MIS 3, because they do not show the more negative source values and thus may have experienced even more evapotranspirative enrichment, possibly caused by elevated temperatures and similar precipitation compared to MIS 3. On the other hand, $\delta^2H_{wax}$ of $nC_{31}$ is much more negative than $nC_{29}$. The reason for this might be different sources of $nC_{29}$ and $nC_{31}$. It makes a difference whether the alkanes are produced by grasses or deciduous trees: grasses produce their *n*-alkanes mainly in the intercalary meristem and are thus much less influenced by evaporative enrichment than deciduous trees and shrubs (Kahmen et al., 2013), which produce their *n*-alkanes mostly at leaf flush (Tipple et al., 2013) and are thus much more influenced by relative hu-

midity. Nevertheless, grasses produce also *n*-alkanes in their leafs (Gao et al., 2012) and also show evaporative enrichment to some degree. In older publications, it has been stated that $nC_{29}$ is mainly produced by deciduous trees (Cranwell, 1973; Zech et al., 2010); the publication of Schäfer et al. (2016a) shows that both $nC_{29}$ and $nC_{31}$ are more or less equally produced by grasses and shrubs. However, relative to $nC_{31}$, Schäfer et al. (2016b) state that deciduous trees produce more $nC_{29}$. Thus the elevated amount of deciduous trees, recorded in the uppermost two samples, might show evaporative enrichment in $nC_{29}$. Also different biosynthetic fractionation of different plants might be a possible influence on the different values (e.g., Gao et al., 2014). As $\delta^2H_{wax}$ values of shrubs, trees and grasses are quite similar (Sachse et al., 2012), we think that evapotranspirative enrichment plays a more important role.

However, it is unclear how changes in atmospheric circulation, and thus source areas, have changed in the past and to which degree a temperature effect at the site of precipitation may have been relevant. If such a temperature effect was relevant on glacial–interglacial timescales and if the isotope record offshore Portugal reasonably reflected changes in the source signal, both effects would have canceled each other out explain the similar $\delta^2H_{precip}$ and $\delta^2H_{wax}$ values during the Holocene and the late MIS 3. Drawing robust paleoclimatological conclusions from $\delta^2H_{wax}$ records thus remains very difficult and independent $\delta^2H_{precip}$ records are needed to reconstruct changes in paleohumidity and evapotranspirative enrichment.

Last but not least, the OEP might also be influenced by climatic conditions: during MIS 3 it is lowest, when $\delta^2H_{wax}$ also has its lowest values. Higher humidity, expressed in lower $\delta^2H_{wax}$ values, might allow higher microbial activity and thus an enhanced degradation, which leads to a lower OEP.

## 6 Conclusions

Our investigations of long-chain *n*-alkanes from the Möhlin sequence reveal that they are well preserved and occur in sufficient amounts in the uppermost samples down to 0.4 m depth, as well as from 1.8 to 5.8 m depth, to use them for the reconstruction of paleovegetation and paleoclimate and for radiocarbon dating. From 0.6 to 1.6 m depth, concentrations are very low, probably related to Holocene pedogenesis and priming.

The *n*-alkane pattern of the uppermost samples reflects today's grassy vegetation and possibly some leaf wax remnants of the natural deciduous forests that prevailed during most of the Holocene. No major vegetation changes are detected below 1.8 m depth. All samples indicate a dominant input of grass-derived leaf waxes and negligible contributions from deciduous trees and shrubs.

Compound-specific $\delta^2H$ analyses have yielded values for the uppermost samples that one can expect from today's isotopic composition of the precipitation, the metabolic fractionation and some evapotranspirative enrichment. The $\delta^2H_{wax}$ values from 1.8 to 5 m depth, i.e., during late MIS 3, are not much different from today's values, which might document that the source effect (more positive source water in the North Atlantic during the glacial) and the temperature effect (more negative precipitation during glacial times) cancel each other out. However, we cannot exclude that changes in evapotranspirative enrichment or in atmospheric circulation and thus source areas were also relevant. Independent records of $\delta^2H_{precip}$ would be necessary to quantitatively derive robust paleoclimatic information, particularly relative humidity and evapotranspirative enrichment. A very interesting feature in the $\delta^2H_{wax}$ pattern from Möhlin is a sudden shift of $\sim 30$ ‰ towards more negative values below 5 m depth. This shift is also observed in another LPS in the northern Alpine foreland and therefore probably a regional phenomenon. It might document a major change in paleohydrology, namely a shift from more humid to more dry conditions at $\sim 32$ ka. Nevertheless, independent $\delta^2H_{precip}$ records are needed for more robust paleoclimatic reconstructions.

Radiocarbon dating of the *n*-alkanes have yielded ages in reasonable agreement with published OSL and IR50 ages, although ages of $\sim 30$ kyr are close to the limit of radiocarbon dating of the *n*-alkanes. The synsedimentary nature and stratigraphic integrity of long-chain *n*-alkanes are thus corroborated, highlighting the great potential of this new tool for dating loess–paleosol sequences. The chronology of the Möhlin sequence shows that loess accumulation occurred during MIS 4 and started again $\sim 34$ ka, well before the onset of MIS 2.

Overall, our study shows the great potential of leaf wax analyses in LPS. More high-resolution records of leaf wax patterns and compound-specific $\delta^2H$, complemented by larger numbers of radiocarbon dating, would be useful to investigate the regional variability of respective proxy patterns. Ideally, such studies should be accompanied by other sedimentological, paleopedological and geochemical methods. Provenance analyses at Möhlin, for example, might help to investigate the proposed changes in wind direction and loess sources. Other leaf wax compounds, such as long-chain *n*-carboxylic acids or n-alkanols, or other biomarkers in general, could be used to corroborate and refine the vegetation reconstruction. Most importantly, the lack of independent $^2H_{precip}$ records currently limits the possibility to robustly reconstruct past changes in relative humidity and evapotranspirative enrichment. A particularly promising path for future work is to further develop the biomarker-based "paleohygrometer", which is based on a coupled $\delta^2H_{wax}$ and $\delta^{18}O_{sugar}$ approach. It allows us to disentangle changes in evapotranspiration and $\delta^2H_{precip}$ and has successfully been tested in topsoils (Tuthorn et al., 2015) and applied to organic-rich archives (M. Zech et al., 2013; Hepp et al., 2015).

**Data availability.** The dataset used in this paper can be found on the Pangaea database (Wüthrich et al., 2017b).

**Competing interests.** The authors declare that they have no conflict of interest.

**Acknowledgements.** We thank Jasmin Aschenbrenner and the Chair of Soil Science, TUM Freising, for support during labwork, Michael Zech and Johannes Hepp for fruitful discussions and the SNF (131670 and 150590) for funding. We also acknowledge the comments of the two reviewers which helped to improve the manuscript.

## References

Abreu, L. de, Shackleton, N. J., Schönfeld, J., Hall, M., and Chapman, M.: Millennial-scale oceanic climate variability off the Western Iberian margin during the last two glacial periods, Mar. Geol., 196, 1–20, https://doi.org/10.1016/S0025-3227(03)00046-X, 2003.

Bowen, G. J. (Ed.): The Online Isotopes in Precipitation Calculator, The GNIP Database, available at: http://www.waterisotopes.org (last access: 17 August 2017), 2008.

Bowen, G. J., Wassenaar, L. I., and Hobson, K. A.: Global application of stable hydrogen and oxygen isotopes to wildlife forensics, Oecologia, 143, 337–348, https://doi.org/10.1007/s00442-004-1813-y, 2005.

Bush, R. T. and McInerney, F. A.: Leaf wax *n*-alkane distributions in and across modern plants: Implications for paleoecology and chemotaxonomy. Geochim. Cosmochim. Ac., 117, 161–179, https://doi.org/10.1016/j.gca.2013.04.016, 2013.

Cranwell, P. A.: Chain-length distribution of *n*-alkanes from lake sediments in relation to post-glacial environmental change, Freshwater Biol., 3, 259–165, https://doi.org/10.1111/j.1365-2427.1973.tb00921.x, 1973.

Dansgaard, W.: Stable isotopes in precipitation, Tellus A, 16, 436–468, 1964.

de Bary, A.: Über die Wachsüberzüge der Epidermis, Botanische Zeitung, 29, 9–11, 1871.

Diefendorf, A. F., Freeman, K. H., Wing, S. L., and Graham, H. V.: Production of *n*-alkyl lipids in living plants and implications for the geologic past, Geochim. Cosmochim. Ac., 75, 7472–7485, https://doi.org/10.1016/j.gca.2011.09.028, 2011.

Drescher-Schneider, R., Jacquat C., and Schoch, C.: Palaeobotanical investigations at the mammoth site of Niederweningen (Kanton Zürich), Switzerland, Quatern. Int., 164–165, 113–129, https://doi.org/10.1016/j.quaint.2006.11.016, 2007.

Eglinton, G. and Hamilton, R. J.: The Distribution of Alkanes, in: Chemical Plant Taxonomy, edited by: Swain, T., Academic Press, London, UK, New York, USA, 187–217, 1963.

Eglinton, G. and Hamilton, R. J.: Leaf Epicuticular Waxes, Science, 156, 1322–1335, https://doi.org/10.1126/science.156.3780.1322, 1967.

Eglinton, T. I. and Eglinton, G.: Molecular proxies for paleoclimatology, Earth Planet. Sc. Lett., 275, 1–16, https://doi.org/10.1016/j.epsl.2008.07.012, 2008.

Farquhar, G. D., Cernusak, L. A., and Barnes, B.: Heavy Water Fractionation during Transpiration, Plant Physiol., 143, 11–18, https://doi.org/10.1104/pp.106.093278, 2007.

Frigola, J., Moreno, A., Cacho, I., Canals, M., Sierro, F. J., Flores, J. A., and Grimalt, J. O.: Evidence of abrupt changes in Western Mediterranean Deep Water circulation during the last 50 kyr: A high-resolution marine record from the Balearic Sea, Quatern. Int., 181, 88–104, 2008.

Gaar, D. and Preusser, F.: Age of the Most Extensive Glaciation of the Northern Switzerland: Evidence from scientific drilling at Möhliner Feld, E&G Quaternary Sci. J., 66, 1–5, https://doi.org/10.3285/eg.66.1.er1, 2017.

Gao, L., Burnier, A., and Huang, Y.: Quantifying instantaneous regeneration rates of plant leaf waxes using stable hydrogen isotope labeling, Rapid Commun. Mass Sp., 26, 115–122, https://doi.org/10.1002/rcm.5313, 2012.

Gao, L., Edwards, E. J., Zeng, Y., and Huang, Y.: Major Evolutionary Trends in Hydrogen Isotope Fractionation of Vascular Plant Leaf Waxes, PloS one, 9, e112610, https://doi.org/10.1371/journal.pone.0112610, 2014.

Gocke, M., Peth, S., and Wiesenberg, G. L.: Lateral and depth variation of loess organic matter overprint related to rhizoliths – Revealed by lipid molecular proxies and X-ray tomography. Landscapes and Soils through Time, Catena, 112, 72–85, https://doi.org/10.1016/j.catena.2012.11.011, 2014.

Gouda, G.: Untersuchungen an Lössen der Nordschweiz, Geogr. Helv., 17, 137–221, https://doi.org/10.5194/gh-17-137-1962, 1962.

Graf, H. R.: Stratigraphie von Mittel- und Spätpleistozän in der Nordschweiz. Beiträge zur Geologischen Karte der Schweiz 168, Bundesamt für Landestopografie swisstopo, Wabern, Switzerland, 2009.

Gutzwiler, A.: Die Diluvialbildung in der Umgebung von Basel. Mitteilungen der naturforschenden Gesellschaft Basel, 10, 512–690, Basel, Switzerland, 1894.

Haas, M., Bliedtner, M., Borodynkin, I., Salazar, G., Szidat, S., Eglinton, T. I., and Zech, R.: Radiocarbon dating of leaf waxes 1 in the loess-paleosol sequence Kurtak, Central Siberia, Radiocarbon, 59, 165–176, https://doi.org/10.1017/RDC.2017.1, 2017.

Haase, D., Fink, J., Haase, G., Ruske, R., Pécsi, M., Richter, H., Altermann, M., and Jäger, K.-D.: Loess in Europe – its spatial distribution based on a European Loess Map, scale 1 : 2 500 000, Quaternary Sci. Rev., 26, 1301–1312, https://doi.org/10.1016/j.quascirev.2007.02.003, 2007.

Häggi, C., Zech, R., McIntyre, C., Zech, M., and Eglinton, T. I.: On the stratigraphic integrity of leaf-wax biomarkers in loess paleosols, Biogeosciences, 11, 2455–2463, https://doi.org/10.5194/bg-11-2455-2014, 2014.

Hepp, J., Tuthorn, M., Zech, R., Mügler, I., Schlütz, F., Zech, W., and Zech, M.: Reconstructing lake evaporation history and the isotopic composition of precipitation by a coupled $\delta^{18}O$–$\delta^{2}H$ biomarker approach. Advances in Paleohydrology Research and Applications, J. Hydrol., 529, 622–631, https://doi.org/10.1016/j.jhydrol.2014.10.012, 2015.

Hoefs, M. J., Rijpstra, W. C., and Sinninghe Damsté, J. S.: The influence of oxic degradation on the sedimentary biomarker record I: evidence from Madeira Abyssal Plain turbidites, Geochim. Cosmochim. Ac., 66, 2719–2735, https://doi.org/10.1016/S0016-7037(02)00864-5, 2002.

Kahmen, A., Schefuß, E., and Sachse, D.: Leaf water deuterium enrichment shapes leaf wax $n$-alkane $\delta$D values of angiosperm plants I: Experimental evidence and mechanistic insights. Hydrogen Isotopes, Geochim. Cosmochim. Ac., 111, 39–49, https://doi.org/10.1016/j.gca.2012.09.003, 2013.

Keller, O. and Krayss, E.: Mittel- und spätpleistozäne Stratigraphie und Morphogenese in Schlüsselregionen der Nordschweiz, E&G Quaternary Sci. J., 59, 88–119, https://doi.org/10.3285/eg.59.1-2.08, 2011.

Kunst, L.: Biosynthesis and secretion of plant cuticular wax, Prog. Lipid Res., 42, 51–80, https://doi.org/10.1016/S0163-7827(02)00045-0, 2003.

Liu, W. and Huang, Y.: Compound specific $D/H$ ratios and molecular distributions of higher plant leaf waxes as novel paleoenvironmental indicators in the Chinese Loess Plateau, Org. Geochem., 36, 851–860, https://doi.org/10.1016/j.orggeochem.2005.01.006, 2005.

Luetscher, M., Boch, R., Sodemann, H., Spötl, C., Cheng, H., Edwards, R. L., Frisia, S., Hof, F., and Müller, W.: North Atlantic storm track changes during the Last Glacial Maximum recorded by Alpine speleothems, Nat. Commun., 6, 6344, https://doi.org/10.1038/ncomms7344, 2015.

Marseille, F., Disnar, J. R., Guillet, B., and Noack, Y.: $n$-Alkanes and free fatty acids in humus and A1 horizons of soils under beech, spruce and grass in the Massif-Central (Mont-Lozère), France, Eur. J. Soil Sci., 50, 433–441, https://doi.org/10.1046/j.1365-2389.1999.00243.x, 1999.

Müller, M. D.: Simulation of thermally induced and synoptically driven wind fields in complex terrain – An evaluation of the mesoscale model MetPhoMod, Master thesis, University of Basel, Basel, Switzerland, 2001.

Penck, A. and Brückner, E.: Die Alpen im Eiszeitalter, 3 Vol., C. H. Tauchnitz, Leipzig, Germany, 1909.

Poynter, J. G., Farrimond, P., Robinson, N., and Eglinton, G.: Aeolian-Derived Higher Plant Lipids in the Marine Sedimentary Record: Links with Palaeoclimate, Springer Netherlands, Dordrecht, the Netherlands, 1989.

Preusser, F., Geyh, M. A., and Schlüchter, C.: Timing of Late Pleistocene climate change in lowland Switzerland, Quaternary Sci. Rev., 22, 1435–1445, https://doi.org/10.1016/S0277-3791(03)00127-6, 2003.

Preusser, F., Graf, H. R., Keller, O., Krayss, E., and Schlüchter, C.: Quaternary glaciation history of northern Switzerland, E&G Quaternary Sci. J., 60, 282–305, 2011.

Ramsey, C. B.: Bayesian Analysis of Radiocarbon Dates, Radiocarbon, 51, 337–360, https://doi.org/10.1017/S0033822200033865, 2009.

Reimer, P. J., Bard, E., Bayliss, A., Beck, J. W., Blackwell, P. G., Ramsey, C. B., Buck, C. E., Cheng, H., Edwards, R. L., Friedrich, M., Grootes, P. M., Guilderson, T. P., Haflidason, H., Hajdas, I., Hatté, C., Heaton, T. J., Hoffmann, D. L., Hogg, A. G., Hughen, K. A., Kaiser, K. F., Kromer, B., Manning, S. W., Niu, M., Reimer, R. W., Richards, D. A., Scott, E. M., Southon, J. R., Staff, R. A., Turney, C. S. M., and van der Plicht, J.: IntCal13 and Marine13 Radiocarbon Age Calibration Curves 0–50 000 Years cal BP, Radiocarbon, 55, 1869–1987, https://doi.org/10.2458/azu_js_rc.55.16947, 2013.

Ruff, M., Fahrni, S., Gaggeler, H. W., Hajdas, I., Suter, M., Synal, H.-A., Szidat, S., and Wacker, L.: On-line Radiocarbon Measurements of Small Samples Using Elemental Analyzer and MICADAS Gas Ion Source, Radiocarbon, 52, 1645–1656, https://doi.org/10.1017/S003382220005637X, 2010.

Sachse, D., Radke, J., and Gleixner, G.: $\delta$D values of individual $n$-alkanes from terrestrial plants along a climatic gradient – Implications for the sedimentary biomarker record, Org. Geochem., 37, 469–483, https://doi.org/10.1016/j.orggeochem.2005.12.003, 2006.

Sachse, D., Billault, I., Bowen, G. J., Chikaraishi, Y., Dawson, T. E., Feakins, S. J., Freeman, K. H., Magill, C. R., McInerney, F. A., van der Meer, Marcel T.J., Polissar, P., Robins, R. J., Sachs, J. P., Schmidt, H.-L., Sessions, A. L., White, J. W., West, J. B., and Kahmen, A.: Molecular Paleohydrology. Interpreting the Hydrogen-Isotopic Composition of Lipid Biomarkers from Photosynthesizing Organisms, Annu. Rev. Earth Pl. Sc., 40, 221–249, https://doi.org/10.1146/annurev-earth-042711-105535, 2012.

Salazar, G., Zhang, Y. L., Agrios, K., and Szidat, S.: Development of a method for fast and automatic radiocarbon measurement of aerosol samples by online coupling of an elemental analyzer with a MICADAS AMS, Nucl. Instrum. Meth. B, 365, 163–167, https://doi.org/10.1016/j.nimb.2015.03.051, 2015.

Samuels, L., Kunst, L., and Jetter, R.: Sealing plant surfaces: cuticular wax formation by epidermal cells, Annu. Rev. Plant Biol., 59, 683–707, https://doi.org/10.1146/annurev.arplant.59.103006.093219, 2008.

Schäfer, I. K., Lanny, V., Franke, J., Eglinton, T. I., Zech, M., Vysloužilová, B., and Zech, R.: Leaf waxes in litter and topsoils along a European transect, SOIL, 2, 551–564, https://doi.org/10.5194/soil-2-551-2016, 2016a.

Schäfer, I. K., Bliedtner, M., Wolf, D., Faust, D., and Zech, R.: Evidence for humid conditions during the last glacial from leaf wax patterns in the loess paleosol sequence El Paraiso, Central Spain, Quatern. Int., 407, 64–73, https://doi.org/10.1016/j.quaint.2016.01.061, 2016b.

Schimmelmann, A., Sessions, A. L., and Mastalerz, M.: Hydrogen isotopic ($D/H$) composition of organic matter during diagenesis and thermal maturation, Annu. Rev. Earth Pl. Sc., 34, 501–533, https://doi.org/10.1146/annurev.earth.34.031405.125011, 2006.

Schlüchter, C., Maisch, M., Suter, J., Fitze, P., Keller, W. A., Burga, C. A., and Wynistorf, E.: Das Schieferkohlenprofil von Gossau (Kt. Zürich) und seine stratigraphische Stellung innerhalb der letzten Eiszeit, Vierteljahrsschrift der Naturforschenden Gesellschaft in Zürich, 132, 135–174, 1987.

Schüepp, W.: Untersuchungen über die Windverhältnisse in der Nordwestschweiz, Geogr. Helv., 37, 208–214, https://doi.org/10.5194/gh-37-208-1982, 1982.

Schwark, L., Zink, K., and Lechterbeck, J.: Reconstruction of postglacial to early Holocene vegetation history in terrestrial Central Europe via cuticular lipid biomarkers and pollen records from lake sediments, Geology, 30, 463–466, https://doi.org/10.1130/0091-7613(2002)030<0463:ROPTEH>2.0.CO;2, 2002.

Sessions, A. L., Burgoyne, T. W., Schimmelmann, A., and Hayes, J. M.: Fractionation of hydrogen isotopes in lipid biosynthesis, Org. Geochem., 30, 1193–1200, https://doi.org/10.1016/S0146-6380(99)00094-7, 1999.

Shepherd, T. and Wynne Griffiths, D.: The effects of stress on plant cuticular waxes, New Phytol., 171, 469–499, https://doi.org/10.1111/j.1469-8137.2006.01826.x, 2006.

Szidat, S., Salazar, G. A., Vogel, E., Battaglia, M., Wacker, L., Synal, H.-A., and Türler, A.: Analysis and Sample Preparation at the New Bern Laboratory for the Analysis of Radiocarbon with AMS (LARA), Radiocarbon, 56, 561–566, https://doi.org/10.1017/S0033822200049602, 2014.

Tarasov, P. E., Müller, S., Zech, M., Andreeva, D., Diekmann, B., and Leipe, C.: Last glacial vegetation reconstructions in the extreme-continental eastern Asia: Potentials of pollen and *n*-alkane biomarker analyses, Quatern. Int., 290–291, 253–263, https://doi.org/10.1016/j.quaint.2012.04.007, 2013.

Tipple, B. J., Berke, M. A., Doman, C. E., Khachaturyan, S., and Ehleringer, J. R.: Leaf-wax *n*-alkanes record the plant–water environment at leaf flush, P. Natl. Acad. Sci. USA, 110, 2659–2664, https://doi.org/10.1073/pnas.1213875110, 2013.

Tuthorn, M., Zech, R., Ruppenthal, M., Oelmann, Y., Kahmen, A., del Valle, H. F., Eglinton, T., Rozanski, K., and Zech, M.: Coupling $\delta^2$H and $\delta^{18}$O biomarker results yields information on relative humidity and isotopic composition of precipitation – a climate transect validation study, Biogeosciences, 12, 3913–3924, https://doi.org/10.5194/bg-12-3913-2015, 2015.

Wang, M., Zhang, W., and Hou, J.: Is average chain length of plant lipids a potential proxy for vegetation, environment and climate changes?, Biogeosciences Discuss., https://doi.org/10.5194/bgd-12-5477-2015, 2015.

Wirsig, C., Zasadni, J., Christl, M., Akçar, N., and Ivy-Ochs, S.: Dating the onset of LGM ice surface lowering in the High Alps, Quaternary Sci. Rev., 143, 37–50, https://doi.org/10.1016/j.quascirev.2016.05.001, 2016.

Wüthrich, L., Garcia Morabito, E., Zech, J., Gnägi, C., Trauerstein, M., Veit, H., Merchel, S., Scharf, A., Rugel, G., Christl, M., and Zech, R.: $^{10}$Be surface exposure dating of the last deglaciation in the Aare Valley, Switzerland, Swiss J. Geosci., accepted, 2017a.

Wüthrich, L., Bliedtner, M., Schäfer, I. K., Zech, J., Shajari, F., Gaar, D., Preusser, F., Salazar, G., Szidat, S., and Zech, R.: *n*-Alkane composition from the Loess Paleosol Sequence Möhlin, Switzerland, PANGAEA, https://doi.org/10.1594/PANGAEA.884114, 2017b.

Zech, M., Buggle, B., Kleiber, K., Marković, S., Glaser, B., Hambach, U., Huwe, B., Stevens, T., Sümegi, P., Wiesenberg, G., and Zöller, L.: Reconstructing Quaternary vegetation history in the Carpathian Basin, SE-Europe, using *n*-alkane biomarkers as molecular fossils, E&G Quaternary Sci. J., 58, 148–155, https://doi.org/10.3285/eg.58.2.03, 2010.

Zech, M., Pedentchouk, N., Buggle, B., Leiber, K., Kalbitz, K., Marković, S. B., and Glaser, B.: Effect of leaf litter degradation and seasonality on D / H isotope ratios of *n*-alkane biomarkers, Geochim. Cosmochim. Ac., 75, 4917–4928, https://doi.org/10.1016/j.gca.2011.06.006, 2011.

Zech, M., Tuthorn, M., Detsch, F., Rozanski, K., Zech, R., Zöller, L., Zech, W., and Glaser, B.: A 220 ka terrestrial $\delta^{18}$O and deuterium excess biomarker record from an eolian permafrost paleosol sequence, NE-Siberia, Chem. Geol., 360–361, 220–230, https://doi.org/10.1016/j.chemgeo.2013.10.023, 2013.

Zech, M., Zech, R., Rozanski, K., Gleixner, G., and Zech, W.: Do *n*-alkane biomarkers in soils/sediments reflect the $\delta^2$H isotopic composition of precipitation? A case study from Mt. Kilimanjaro and implications for paleoaltimetry and paleoclimate research, Isot. Environ. Healt. S., 51, 1–17, https://doi.org/10.1080/10256016.2015.1058790, 2015.

Zech, M., Kreutzer, S., Zech, R., Goslar, T., Meszner, S., McIntyre, C., Häggi, C., Eglinton, T. I., Faust, D., and Fuchs, M.: Comparative $^{14}$C and OSL dating of loess-paleosol sequences to evaluate post-depositional contamination of *n*-alkane biomarkers, Quaternary Res., 87, 180–189, https://doi.org/10.1017/qua.2016.7, 2017.

Zech, R., Zech, M., Marković, S., Hambach, U., and Huang, Y.: Humid glacials, arid interglacials? Critical thoughts on pedogenesis and paleoclimate based on multi-proxy analyses of the loess–paleosol sequence Crvenka, Northern Serbia, Palaeogeogr. Palaeocl., 387, 165–175, https://doi.org/10.1016/j.palaeo.2013.07.023, 2013.

Zech, R., Mayr, C., and Doppler, G.: Löss und Paläoböden in Bobingen. Eine geochemische Reise in die letzte Eiszeit, in: DBG Mitteilungen, edited by: Auerswald, K. und Ahl, C., Bd. 117: Deutsche bodenkundliche Gesellschaft, München, Germany, 139–148, 2015.